PROCEEDINGS, Sixteenth Workshop on Geothermal Reservoir Engineering
Stanford University, Stanford, California, January 23-25, 1991
SGP-TR-134

SIMULATING WELLFLOW OF HIGH-NONCONDENSABLE-GAS GEOFLUIDS USING LABORATORY MEASUREMENTS ON SECONDARY FLUIDS

LAOULACHE, R.N. AND DIPIPPO, R.

MECHANICAL ENGINEERING DEPARTMENT
SOUTHEASTERN MASSACHUSETTS UNIVERSITY
NORTH DARTMOUTH, MA 02747

ABSTRACT

An experimental simulation of an actual steam-water geothermal well based on field data obtained in New Zealand is carried out in a two-phase flow facility using dichlorotetrafluoroethane, known commercially as refrigerant 114. The simulation of steam-water flow is accomplished by a similarity theory which is achieved by using appropriate dimensionless numbers; namely, the Mach, Froude, and Reynolds numbers at the flashing front. The theory is used to scale the flow properties from that of water to that of refrigerant 114 in the two-phase region, and permits the prediction of steam-water characteristics in a flowing well, under much reduced pressure and temperature levels. Two experimental series were conducted to confront the similarity theory with actual measurements from a flowing well with significant noncondensable gases. Experimental results using refrigerant 114 indicate that the pressure distribution along the pipe can be predicted accurately in the two-phase region of a geothermal well.

NOMENCLATURE

a	sonic velocity (m/s)
A	distribution coefficient
C	specific heat (kJ/kg/^{o}C)
D	pipe diameter (m)
F	mass fraction of noncondensable gas
Fr	Froude number
g	acceleration of gravity (m/s^2)
h	enthalpy (kJ/kg)
K	Henry's constant (atm)
$\dot{m}$	mass flow rate (m/sec)
M	molecular weight (g/gmole)
Ma	Mach number
n	number of moles (gmole)
N_D	similarity parameter
P	pressure (bar,a)
Re	Reynolds number
R_a	apparent gas constant (kJ/kg/^{o}C)
T	temperature (K)
v	specific volume (m^3/kg)
x	dryness fraction
X	mole fraction
z	height from flashing front (m)
W	velocity (m/s)
ψ	mass flux (kg/m^{2}s)
μ	dynamic viscosity (Pa.s)

Subscript

a	apparent
c	carbon dioxide CO_2
f	liquid
fg	evaporation/condensation
g	gaseous phase
M	measured
meas	measured
o	stagnation condition
or	orifice
r	refrigerant R-114
ref	reference
res	reservoir
sat	saturation condition
T	total
v	vapor
w	water H_2O

Superscript

*	flashing condition

BACKGROUND

In the mid 1980s the U.S. Department of energy funded a research project at Brown University aimed at developing a reliable, safe, predictive and relatively inexpensive method of simulating the two-phase flow of geothermal fluids in a controlled laboratory environment. The working fluid for the laboratory studies would not be water (due to the high temperatures and pressures) but a fluid that would simulate water (a similarity fluid).

The concept of similitude (or scaling) is well-established for single-phase flows, but is less for two-phase, liquid-vapor flows. This study should not be confused with other studies whose goal is to model actual two-phase flows, particularly in geothermal wells [1-4]. The theoretical basis for the Brown University study, and details of the laboratory setup are given in Refs. [5-6].

The fundamental premise for this effort is depicted schematically in Figure 1. A reliable and predictive similarity theory provides laws for all physical variables pertaining to the problem. These include, in this case, pipe diameters and lengths, fluid flow rates, temperatures and pressures. Expensive, cumbersome, risky and inaccurate field measurements may thus be replaced with relatively inexpensive, controlled, safe and highly accurate laboratory experiments. Having in hand the analytical tools to relate the laboratory results to field results, one may easily design the field equipment (surface piping as well as production and injection wells) for optimum characteristics.

In this paper, we offer a brief summary of the basic similarity theory developed by the Brown University team. The case of geofluids with significant amounts of noncondensable gas is examined through the use of the laws of Henry and Raoult. The experimental facility is described as it

existed at Brown University and the results of a series of measurements designed to prove out the theory are presented.

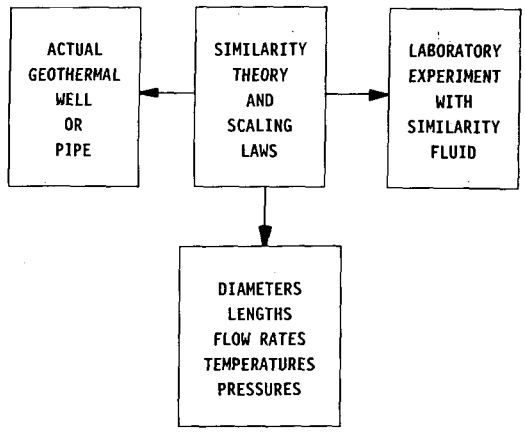

Figure 1. Basic Concept of laboratory simulation of geothermal fluid flow

SUMMARY OF SIMILARITY THEORY

Basic Theory

Many similarity theories have been proposed in two-phase flows [7-10] to simulate water-steam mixtures using fluorinated hydrocarbons. In this work no attempt is made to test these theories since our experimental arrangement required certain reference parameters which differ markedly from other proposed criteria. The reference groups which we identified as the important controlling inlet conditions for pipe flow [11-12] are the Mach, Froude, and Reynolds numbers (Ma^*, Fr^*, Re^*) at the flashing front defined as:

$$Ma^* = W_f^*/a^* \quad (1)$$

$$Fr^* = W_f^*/(g\,D)^{1/2} \quad (2)$$

$$Re^* = \psi\, D/\mu^* \quad (3)$$

$$\text{where } W_f^* = \psi\, v_f^* = (\dot{m}/A)\, v_f^*. \quad (4)$$

The sonic velocity a^* is avaluated under the assumption that the two-phase flow mixture at flashing is homogeneous [13].

In an earlier work [5] we developed a similarity theory to relate reference parameters for R-114 with those of water-steam mixtures. Here we will only summarize the theory. The basic assumptions are the following:

$$1)\ v_f = \text{constant}. \quad (5)$$

$$2)\ h_{fg} = h_g - h_f = \text{constant}. \quad (6)$$

3) Saturated vapor phase obeys the perfect gas equation of state:

$$P\, v_g = R_a\, T, \quad (7a)$$

$$\text{or } P\, v_{fg} = R_a\, T \quad (7b)$$

since in general, $v_g >> v_f$.

These assumptions are valid for water substance over the range 100-300°C and for R-114 in the range of -20 to 70°C.

With the appropriate choice of reference parameters, the theory shows that the temperature, pipe diameter and height correspondences between water substance and R-114 are given by:

$$(T_r/T_w) = (h_{fg,r}\, R_{a,w})/(h_{fg,w}\, R_{a,r}), \quad (8)$$

$$(D_r/D_w) = (T_r\, C_{f,r})/(T_w\, C_{f,w}), \quad (9)$$

$$\text{and } (z_w/z_r) = (D_w/D_r) \quad (10)$$

respectively. At the flashing front, similarity requires that

$$Ma_w^* = Ma_r^*, \quad (11)$$

$$\text{and } Fr_w^*/Fr_r^* = N_{D,w}/N_{D,r}, \quad (12)$$

where

$$N_D = (P\, v_f\, R_a/h_{fg}/C_f)\ e^{(T\, R_a/h_{fg})}. \quad (13)$$

The whole idea can be summarized in the following way. From the stagnation temperature in the reservoir (= flash temperature under adiabatic conditions), the mass flow rate of water, together with the pipe diameter, one can determine the required flash temperature, pipe diameter, and the mass flow rate of R-114 to simulate the steam-water conditions using this similarity theory. Then, the results of tests on the R-114 under controlled laboratory conditions can be used to predict the temperature and pressure of steam-water mixtures in an actual vertical flow. According to eqs.(8-9), to simulate a case where water, flowing at 42 kg/s, flashes at 250°C in a 15 cm pipe, for example, R-114 would have to be flowing at 0.2 kg/s, and flashing at a temperature of 45.4°C in a 2 cm pipe.

If one measures the temperature of R-114, T_r, along the test section, then the temperature T_w for water-steam mixture can be calculated from eq. (8), and the saturation pressure P_w can be found from standard steam tables.

The accuracy of the predicted pressure P_w in the two-phase region can be tested by a comparison with actual pressure measurements from field data.

Noncondensable Gas Effects

Since most geothermal fluids carry noncondensable gases (mostly carbon dioxide, CO_2), it is necessary to investigate this effect. A thermodynamic analysis based on phase equilibrium between water-steam mixtures and CO_2 at any temperature shows that the latter behaves as a solute in a dilute liquid solution of H_2O. If we treat H_2O as an ideal solution, then we can use Henry's law which states that the partial pressure of CO_2 is given by:

$$P_c = K_c\ X_c, \quad (14)$$

where X_c is the mole fraction of CO_2 in the liquid phase of the steam-water mixture:

$$X_c = n_{c,f}\ /\ (n_{c,f} + n_{w,f}). \quad (15)$$

Henry's constant can be found in Ref. [14]. Using the distribution coefficient A [15], the ratio of moles of CO_2 in the liquid phase to that in the vapor phase can be expressed as:

$$(n_{c,f}/n_{c,v}) = A\ (n_{w,f}/n_{w,v}). \quad (16)$$

In the vapor phase:

$$\dot{n}_{c,v} = \dot{m}_{c,v} / M_c \quad (17)$$

$$\dot{n}_{w,v} = \dot{m}_{w,v} / M_w. \quad (18)$$

Of the total mass flow rate $\dot{m}$, the mass flow rates of CO_2 gas and water-steam mixture are:

$$\dot{m}_{c,v} = F\,\dot{m} \quad (19)$$

$$\dot{m}_w = (1 - F)\,\dot{m}, \quad (20)$$

respectively. F is the mass fraction of noncondensable gases. The fraction of $\dot{m}_w$ that is vapor can be determined in terms of the dryness fraction x in the absence of CO_2; that is,

$$\dot{m}_{w,v} = x\,\dot{m}_w. \quad (21)$$

Hence, eq.(15) can be written in terms of eqs.(16-21) as:

$$X_c = [1 + x(1-F)M_c/(A\,F\,M_w)]^{-1}. \quad (22)$$

The dryness fraction x can be calculated from the energy balance between the stagnation point and any section in the two-phase region, for an adiabatic well. Refs. [11,16] show that the kinetic and potential energies per unit mass are negligible in comparison to the latent heat of evaporation. In this case, the dryness fraction is given by:

$$x = (h_o - h_f)/h_{fg}. \quad (23)$$

From Raoult's law, the pressure of liquid water is given by:

$$P_{w,f} = P_{w,sat}\ X_{w,f}, \quad (24)$$

where $X_{w,f} = 1 - X_c$. (25)

The total calculated pressure is

$$P_T = P_{w,f} + P_c. \quad (26)$$

EXPERIMENTAL FACILITY

The experimental work was conducted at Brown University [17] where a facility was designed specifically to study two-phase flow of single substance with phase change, and to simulate flow conditions in geothermal wells. A schematic of this computer-controlled facility is shown in Figure 2. The test section is shown vertical and lies between two isolation butterfly valves (BFV-D and BFD-U) as shown in Figure 3. The working fluid is dichlorotetrafluoroethane (CCl_2F-CCl_2F) known as refrigerant 114 (R-114). The temperature and absolute pressure are measured at the inlet of the test section (stagnation point). Along the test section, the temperature and differential pressure are measured at four stations, 1.219 m apart.

Opening the two butterfly valves initiates the flow in the upward direction under the pressure difference between the accumulator and the condenser. When the gate valve (GV) is slightly open, the fluid flows as single-phase liquid up to and past an orifice plate at the inlet of the test section, and flashes somewhere in the test section to form a two-phase flow. Adjusting the opening of the GV with a computerized servomotor varies the degree of flashing in the test section by changing the back pressure on the orifice plate.

Between the two extreme positions of the GV, a sequence of flows with different topologies can be generated in the test section that would otherwise occur in different positions along a much longer pipe, starting with bubbly flow near flashing that changes ultimately to an annular flow as the GV is progressively opened.

Thus, if we imagine that the fixed test section can be "shifted" in the flow direction, then the set of data can be essentially "pieced" together to represent temperature, and pressure distributions along a very long pipe [11].

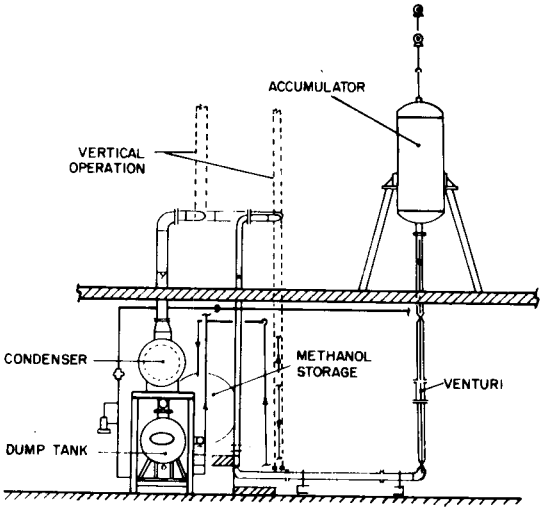

FIGURE 2 VERTICAL SECTION OF THE TEST FACILITY

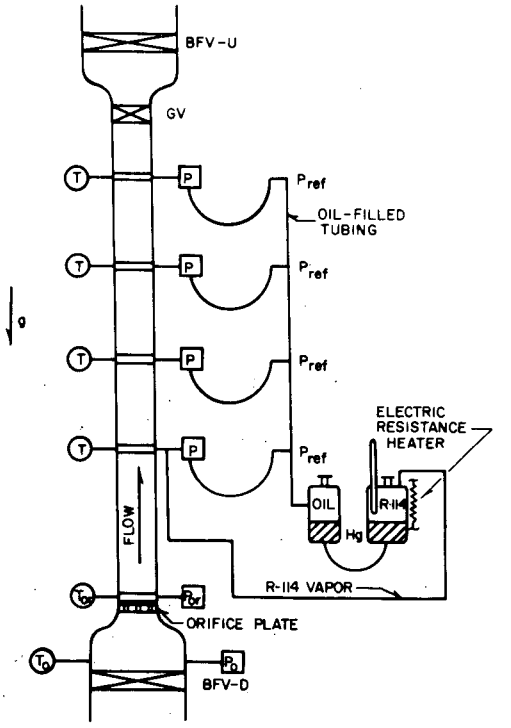

FIGURE 3 VERTICAL TEST SECTION CONFIGURATION

In this experiment a commercially available copper tube was used and it was completely insulated. In order to accurately determine the position of the flash front four additional thermistors, 0.457 m apart, were added along the test section. The first thermistor was at 0.910 m from the stagnation point near the BFV-D.

MEASUREMENTS AND RESULTS

Survey of Well Field Data

We have collected data on wellflow characteristics from a number of wells in New Zealand [18]. They include KA (10,16) (Kawerau); NG (3,9,11,12,13) (Ngahwa); and BR (11,21) (Broadlands/Ohaaki). Geofluid parameters are given in columns 2-4 in Table 1.

TABLE 1

SIMILARITY CONDITIONS FOR SELECTED WELLS

	GEOFLUID					REFRIGERANT-114				
Well No.	D cm	T °C	$\dot{m}$ kg/s	Ma*	Fr*	D cm	T °C	$\dot{m}$ kg/s	Ma*	Fr*
KA-10	15.04	250	42.0	0.105	2.437	2.00	45.4	0.202	0.107	1.037
KA-16	15.04	248	19.0	0.049	1.098	2.01	44.3	0.092	0.049	0.469
NG-3	15.04	228	20.0	0.068	1.117	2.04	33.7	0.104	0.069	0.496
NG-3	15.04	228	24.4	0.083	1.362	2.04	33.7	0.127	0.084	0.605
NG-11	19.88	224	64.4	0.133	1.779	2.71	31.6	0.340	0.134	0.797
NG-11	19.88	224	68.8	0.142	1.895	2.71	31.6	0.362	0.142	0.849
NG-12	19.88	228	13.3	0.026	0.370	2.70	33.7	0.069	0.026	0.164
NG-13	22.05	225	19.4	0.032	0.414	3.00	32.1	0.102	0.032	0.185
NG-13	22.05	225	53.0	0.088	1.131	3.00	32.1	0.280	0.088	0.506
BR-11	19.88	240	62.2	0.102	1.765	2.68	40.1	0.311	0.103	0.765
BR-21	19.88	260	21.9	0.028	0.645	2.61	50.5	0.100	0.028	0.270
BR-21	19.88	260	26.1	0.033	0.769	2.61	50.5	0.120	0.033	0.321

The stagnation temperature of most wells is very high which leads to a relatively high stagnation temperature even under laboratory conditions, as our similarity theory requires (column 8 in Table 1). The instrumentation however was not designed for stagnation temperatures much higher than 30°C for R-114. Unfortunately, field data with low stagnation temperatures were not available. Hence, we settled on one set of data obtained in a well identified as NG-11.

The characteristics of well NG-11 are given in Table 2 and 3. The 1.4 % gas content of the total mass flow rate represents noncondensable gases that are greater than 95 % CO_2 [18]. From the data of Table 3 it appears that the difference between the measured pressure (above the flashing front), and the saturation pressure is due to the partial pressure of carbon dioxide present as a noncondensable gas. To check this observation, let us analyze the two-phase region which consists of a mixture of steam-water and carbon dioxide gas.

TABLE 2

CHARACTERISTICS OF WELL NG-11

Reservoir temperature, T (°C)	224.0
Reservoir pressure, P_{res} (bar,a)	93.0
Stagnation enthalpy (kJ/kg)	965
Mass flow rate, $\dot{m}$(kg/s)	64.4
Noncondensable gas content	
NGC/% totalflow (by mass)	1.4

TABLE 3

PRESSURE AND TEMPERATURE AS A FUNCTION OF DEPTH FOR WELL NG-11

Depth (m)	T_{meas} (°C)	P_{meas} (bar,a)	$P_{H_2O,sat}$ (bar,a)
0	206	20.0	17.65
100	211.5	23.5	19.67
200	215	27.5	21.12
300	218.5	32.0	22.56
400	220	38.0	23.18
500	222.5	44.8	24.20
600	223.5	52.9	24.70
700	224	61.1	25.00

Note: $P_{H_2O,sat}$ was calculated from Steam Tables at the measured temperature.

Table 4 shows the values of parameters which lead to the predicted total pressure P_T. The data clearly indicates that equations (14-26) give an accurate description of the pressure distribution P_M along the pipe. There is strong agreement with the measured pressures between 0-400 m. However, the calculated pressure disagrees with the measured pressure at a depth of 500 m. This means that the flash front lies between 400 and 500 m. Figure 4 shows the temperature profile along the pipe as a function of depth. It can be seen that temperature points at depth greater than 400 m have a steeper slope than points shallower than 400 m. We will assume that flashing occurs at a depth of 400 m. At depths greater than 400 m, the mixture is compressed liquid.

The analysis above shows that the vapor pressure of water can be separated from that of carbon dioxide according to the laws of Henry and Raoult. This is an important result since the similarity theory which is being tested was developed for pure substances in the absence of any noncondensable gases. This means that the pressure similarity is between the saturation pressure of the laboratory fluid (R-114) and the partial pressure of water vapor rather than the total pressure of the water-steam and carbon dioxide mixture.

TABLE 4

PREDICTED PARTIAL VAPOR PRESSURE AND TOTAL PRESSURE AS A FUNCTION OF DEPTH FOR WELL NG-11

Depth (m)	0	100	200	300	400	500
T_{meas} (°C)	206	211.5	215	218.5	220	222.5
K_{CO_2} (atm)	6280	6170	6100	6030	6000	5950
1/A	327	286	262	240	231	217
x 10^2	4.38	3.09	2.25	1.42	1.11	0.53
X_{CO_2} 10^4	4.05	6.57	9.85	17.01	22.60	50.25
P_{CO_2} (bar,a)	2.58	4.11	6.10	10.41	13.76	30.34
P_{H_2O} (bar,a)	17.64	19.66	21.10	22.52	23.13	24.08
P_T (bar,a)	20.22	23.77	27.20	32.93	36.89	54.42
P_M (bar,a)	20.0	23.5	27.5	32.0	38.0	44.80

Note: P_{CO_2} was calculated from Henry's law; P_{H_2O} was found from Raoult's law.

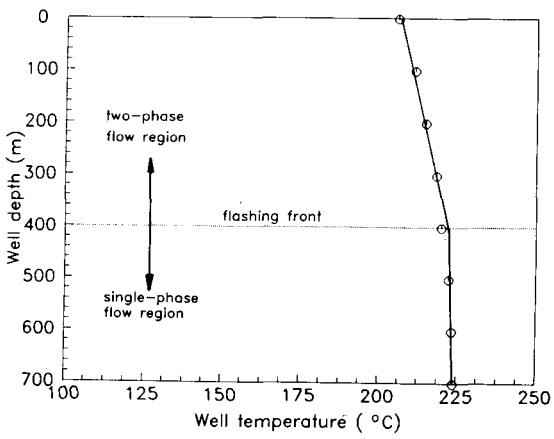

Figure 4. Temperature profile for WELL NG-11

Method of Testing

From the reservoir temperature, mass flow rate, and pipe diameter of well NG-11, we calculated the mass flux, flash Mach, Froude, and Reynolds numbers. This is shown in row 1 of Table 5. Similarity theory requires a constant flashing Mach number, and scaled temperature and diameter for R-114 based on eqs.(8-9). The matching conditions for R-114 are shown in row 2 of Table 5.

TABLE 5

SIMILARITY BETWEEN WATER AND R-114

		T(°K)	$\dot{m}$(kg/s)	D(m)	ψ(kg/m^{2}s)	Ma^*	Fr^*	Re^*x10^{-3}
1.	Water[1]	497.16	64.4	0.1988	2075	0.134	1.779	3461
2.	R-114[2]	304.72	0.34	0.0271	589	0.134	0.797	50.07
3.	R-114 Test (Series 5)	304.36	0.34	0.0254	671	0.156	0.940	53.65
4.	%Uncertainty	±0.13	±0.50			±1.0	±0.51	±0.70
5.	%Deviation Between Rows 2 & 3	0.12	0.0	-6.3	13.9	16.4	17.9	7.1
6.	R-114 Test (Series 6)	304.03	0.292	0.0254	576	0.134	0.801	45.46
7.	% Uncertainty	±0.02	±0.99			±1.0	±1.0	±0.70
8.	%Deviation Between Rows 2 & 6	-0.23	-14.0	-6.3	-2.2	0.0	0.5	-9.2

(1)Data taken from well NG-11; (2)According to similarity theory.

Under laboratory conditions, similarity requires a pipe of 0.0271 m. Due to the difficulty of finding a commercial pipe of exactly 0.0271 m, it was decided to use a 0.0254 m commercially available copper tube.

Using this tube, a series of 27 experiments (called Series 5) were conducted under fixed flashing conditions and mass flow rate, with a very small experimental uncertainty. Row 4 shows the uncertainty (in percent) in holding flashing conditions constant for Series 5. From the data it can be seen that the flash temperature and mass flow rates deviate by 0.12% and 0% from what is required. However, the discrepancy of 6.3% in the diameters resulted in large deviations in the flash Mach number Ma^*, and the Froude number Fr^*, as seen in row 5 of Table 5. In an attempt to compensate for the diameter discrepancy, the mass flux was scaled rather than the mass flow rate. From the data in Table 5, similarity requires a mass flux of 589 kg/(m^{2}s), whereas the actual measured mass flux in the laboratory is 671 kg/(m^{2}s) in Series 5. In a 0.0254 m pipe, a mass flux of 589 kg/(m^{2}s) would require a mass flow rate of 0.30 kg/s instead of 0.34. Thus, a new series of tests (Series 6) was carried out to correct for the discrepancies in Series 5. The measured parameters in Series 6 are shown in row 6 along with the experimental uncertainty in row 7. As can be seen from row 8, Series 6 meets the similarity requirements for mass fluxes rather than mass flow rates.

Laboratory Results versus Field Data

Results of measured temperatures for Series 5 only are shown in Table 6A; measurements of Series 6 are nearly identical, as we will see. Temperature measurements from only the top three probes are considered (Fig. 3) since they are the furthest from the flashing front.

It is interesting to note that the method of "piecing" measurements together is a very convenient way to predict conditions for a long pipe using a much shorter pipe in the laboratory. For example, in row 7, the probe for T_2 is 9.36 m from the flashing front, for a given GV opening, and the measured temperature is 20.4°C. As the GV is opened further, the flashing front moves upstream toward the orifice plate and away from the T_2-probe. But the T_1-probe is now at 9.35 m as shown in row 8. Notice that at essentially the same distance from z^*, the T_1-probe reads 20.43°C, approximately the same as the T_2-probe at the previous GV setting.

Using the measured temperatures T_1, T_2, and T_3 of R-114 from Series 5 and 6, the temperatures and heights of water-steam mixtures are calculated from eqs.(8) and (10) respectively. Values from Series 5 are shown in Table 6B.

TABLE 6A

EXPERIMENTAL TEMPERATURES AND HEIGHTS FOR R114 - SERIES 5

z_1 (m)	z_2 (m)	z_3 (m)	T_1 (°C)	T_2 (°C)	T_3 (°C)
1.22	2.44	3.66	26.89	25.65	24.60
2.21	3.43	4.65	25.88	24.86	23.84
3.14	4.36	5.58	25.10	24.12	23.16
6.26	7.48	8.70	22.65	21.70	20.87
7.10	8.32	9.54	22.00	21.16	20.25
7.79	9.01	10.23	21.52	20.64	19.69
8.14	9.36	10.58	21.27	20.40	19.57
9.35	10.57	11.78	20.43	19.56	18.66
12.02	13.24	14.46	18.51	17.61	16.80
12.11	13.33	14.55	18.42	17.59	16.72
13.19	14.41	15.63	17.65	16.81	15.97
14.63	15.85	17.07	16.66	15.78	14.94
15.45	16.67	17.89	16.07	15.18	14.27
16.16	17.38	18.60	15.55	14.66	13.79
16.73	17.95	19.17	15.13	14.22	13.32
18.14	19.35	20.57	14.09	13.14	12.21
19.11	20.33	21.55	13.33	12.33	11.33
20.21	21.43	22.65	12.43	11.37	10.35
21.83	23.05	24.26	11.05	9.95	8.84
24.36	25.58	26.80	8.89	7.80	6.54
24.69	25.91	27.13	8.59	7.50	6.28
24.81	26.03	27.24	8.49	7.40	6.12
26.93	28.14	29.36	6.43	5.33	3.98
29.17	30.38	31.60	4.18	2.94	1.44
29.28	30.50	31.72	4.06	2.88	1.46
29.40	30.62	31.84	3.95	2.77	1.35
39.63	30.85	32.07	3.72	2.51	1.06

Note: z_1, z_2, z_3 are measured relative to the flashing front ($z^* = 0$).

TABLE 6B

PREDICTED TEMPERATURES AND HEIGHTS FOR STEAM-WATER MIXTURE FROM TABLE 6A BASED ON SIMILARITY THEORY

z_1 (m)	z_2 (m)	z_3 (m)	T_1 (°C)	T_2 (°C)	T_3 (°C)
8.94	17.89	26.84	216.30	214.28	212.57
16.24	25.18	34.13	214.65	212.99	211.33
23.08	32.02	40.97	213.38	211.78	210.22
45.97	54.92	63.86	209.39	207.84	206.48
52.09	61.04	69.99	208.33	206.95	205.47
57.20	66.15	75.10	207.54	206.11	204.56
59.75	68.69	77.64	207.13	205.72	204.36
68.59	77.53	86.48	205.76	204.34	202.88
88.25	97.19	106.14	202.63	201.16	199.84
88.86	97.81	106.76	202.49	201.13	199.71
96.82	105.76	114.71	201.23	199.86	198.49
107.36	116.31	125.26	199.61	198.18	196.81
113.36	122.31	131.76	198.65	197.20	195.72
118.59	127.54	136.48	197.80	196.35	194.92
122.81	131.76	140.71	197.12	195.63	194.17
133.09	142.04	150.99	195.42	193.87	192.36
140.25	149.20	158.15	194.18	192.55	190.92
148.30	157.25	166.20	192.71	190.98	189.32
160.18	169.12	178.07	190.46	188.67	186.86
178.77	187.71	196.66	186.94	185.16	183.11
181.77	190.17	199.12	186.45	184.67	182.68
182.05	191.00	199.94	186.29	184.51	182.42
197.60	206.55	215.50	182.93	181.13	178.93
214.04	222.98	231.93	179.26	177.23	174.79
214.90	223.85	232.80	179.06	177.14	174.82
215.74	224.68	233.63	178.88	176.96	174.64
217.48	226.43	235.38	178.51	176.53	174.17

Note: z_1, z_2, z_3 are measured relative to the flashing front ($z^* = 0$).

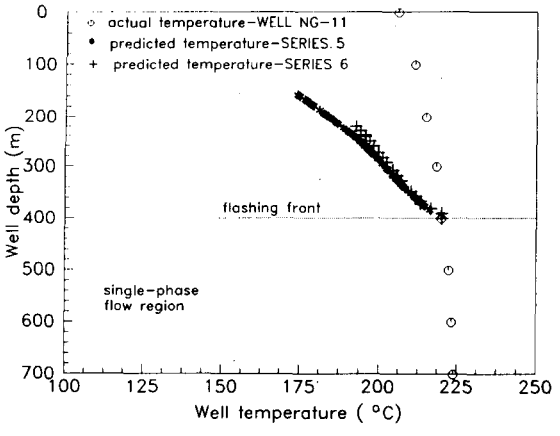

Figure 5. Predicted and actual temperature profiles for WELL-NG 11

DISCUSSION

A comparison of predicted and actual temperatures is shown in Figure 5, with average and maximum relative deviations of 5% and 9% respectively. However, the comparison is more reasonable when we compare pressures.

From the predicted temperatures of steam-water in Table 6B, the partial pressures are calculated from standard steam tables. The result is shown in Figure 6. Two observations should be made. The first one is that the predicted partial pressure at flashing is below the actual pressure by exactly the partial pressure of CO_2 at the flashing front. The second observation is that the predicted pressure gradients for Series 6, away from flashing, is within 3% of that in the actual well as shown in Figure 7. This indicates that if CO_2 were not present, the predicted pressure would be coincident with the actual pressure at the flashing front, and would develop with a pressure gradient deviating by 3% from the actual one. The effect of the presence of CO_2 is to suppress the whole predicted pressure curve by an amount equal to the pressure of CO_2 at flashing. By adding the partial pressure of CO_2 at flashing to the predicted pressure, then the calculated total pressure and the actual pressure in the well will be identical at the flashing front as shown in Figure 8.

From Figure 8, the agreement between the predicted pressure and the actual pressure of water in the well is very good if the predicted and actual pressures are anchored at the flashing front as required by the similarity theory.

It is worth noting that the attempt to correct for the diameter discrepancy By matching the mass flux resulted in a mass flow rate in Series 6, 14% lower than that in Series 5. This effect decreased the initial acceleration pressure gradient at the flash front (Fig. 7), and the pressure became closer to the actual one in the well.

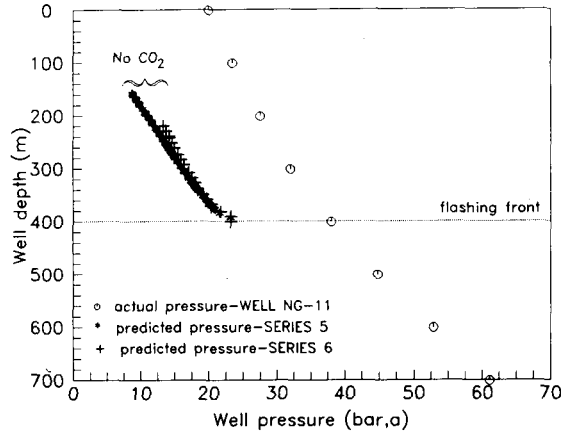

Figure 6. Predicted and actual pressure profiles for WELL-NG 11

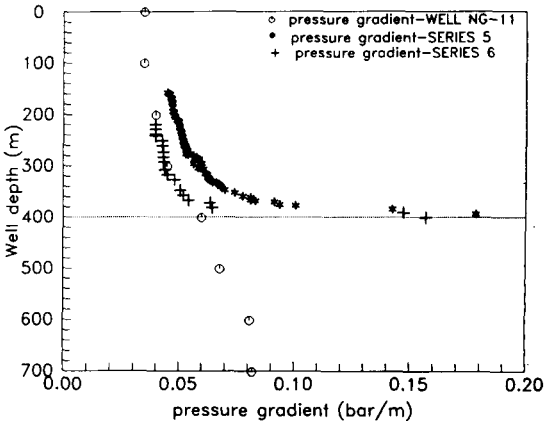

Figure 7. Predicted and actual pressure gradient profiles for WELL NG-11

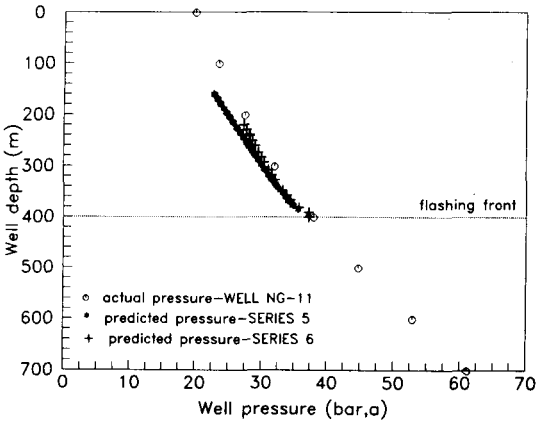

Figure 8. Predicted and actual pressure profiles for WELL-NG 11

CONCLUSION

In this study we showed that a similarity theory can be used successfully in the presence of significant noncondensable gases, to predict the pressure along a vertical pipe of an adiabatic geothermal well. The input field data required for laboratory simulation using R-114 are the mass flow rate of water, the pipe diameter, the stagnation pressure and temperature, and mass fraction of noncondensable gases. From this information, flashing conditions under laboratory conditions are established from similarity theory, and measurements are conducted under those conditions. From the measurements, the partial pressure of water is predicted using similarity theory. The contribution of the partial pressure of CO_2 at flashing is calculated using Henry's law. Hence, the total pressure in the two-phase region, as well as the height above the flashing front can be predicted.

REFERENCES

[1] Barelli, A., Corsi, R., DelPizzo, G., and Scali, C., "A Two-Phase Flow Model for Geothermal Wells in the Presence of Non-Condensable Gas," **Geothermics**, v. 11, no. 3, 1982, pp. 175-191.

[2] Michaelides, E. E., and Shafaie, F. F., "A Numerical Study of Geothermal Well Flow with Salts and Noncondensables present," **Trans. ASME**, v. 108, 1986, pp. 140-145.

[3] Freeston, D. H., and Hadgu, T., "Modelling of Geothermal Wells with Multiple Feed Points: A Preliminary Study,"**Proc. 9th NZ Geoth. Workshop**, 1987, pp. 59-64.

[4] Hadgu, T., and Freeston, D. H., "A Multipurpose Wellbore Simulator," **GRC TRANS.**, v. 14, pt. II, 1990, pp. 1279-1286.

[5] Maeder, P. F., DiPippo, R., Dickinson, D. A., and Nikitopoulos, D. E., "Modelling of Flashing Flows Using Similarity Fluids," **Fundamental Aspects of Gas-Liquid Flows**, Michaelides, E. E., ed., FED-v. 29, 1985, pp. 109-116.

[6] Maeder, P. F., Dickinson, D. A., Nikitopoulos, D. E., and DiPippo, R., "A Facility for the Experimental Investigation of Single Substance Two-Phase Flow," **Fundamental Aspects of Gas-Liquid Flows**, Michalides, E. E., ed., FED-v. 29, 1985, pp. 41-46.

[7] Mayinger, F., "Scaling and Modelling Laws in Two-Phase Flow and Boiling Heat Transfer," **Two-Phase Flow and Heat Transfer**, Vol. 1, Kakac, S., and Veziroglu, T. N., eds., Hemisphere Pub. Corp., Washington, DC, 1976, pp. 129-161.

[8] Ishii, M., and Jones, O. C., Jr., "Derivation and Application of Scaling Criteria for Two-Phase Flows," **Two-Phase Flow and Heat Transfer**, Vol. 1, Kakac, S., and Veziroglu, T. N., eds., Hemisphere Pub. Corp., Washington, DC, 1976, pp. 163-185.

[9] Fridel, L., "Momentum Exchange and Pressure Drop in Two-Phase Flow," **Two-Phase Flow and Heat Transfer**, Vol. 1, Kakac, S., and Veziroglu, T. N., eds., Hemisphere Pub. Corp., Washington, DC, 1976, pp. 239-312.

[10] Kowalczewski, J. J., "Two-Phase Flow in an Unheated and Heated Tubes," Dissertation ETH, Zurich, 1964.

[11] Nikitopoulos, D. E., and Maeder, P. F., "Single-Substance Two-Phase Flow: A Unified Theoretical and Experimental Study," Brown University, Report no. TWOPHASE/3, 1986, Providence, RI.

[12] Dickinson, D. A., and Maeder, P. F., "An Investigation of Single Substance Horizontal Two-Phase Flow," Brown University, Report no. GEOFLO/20, 1984, Providence, RI.

[13] Maeder, P. F., DiPippo, R., Delor, M., and Dickinson, D., "The Physics of Two-Phase Flow: Choked Flow," Brown University, Report no. GEOFLO/10, May 1981, Providence, RI.

[14] Ellis, A. J., and Golding, R. M., "The Solubility of Carbon Dioxide Above 100 °C in Water and in Sodium Chloride Solutions," **American Journal of Science**, v. 261, Jan 1963, pp. 47-60.

[15] Ellis, A. J., "The Solubility of Carbon Dioxide in Water at High Temperatures," **American Journal of Science**, v. 257, Mar 1959, pp. 217-234.

[16] Delhaye, J. M., Giot, M., and Riethmuller, M. L., **Thermohydraulics of Two-Phase Systems for Industrial Design and Nuclear Engineering**, Hemisphere Publishing Corp., 1981, pp. 428.

[17] Laoulache, R. N., Maeder, P. F., and DiPippo, R., "Theoretical and Empirical Study of Single-Substance, Upward Two-Phase Flow in a Constant-Diameter Adiabatic Pipe," Brown University, Report no. TWOPHASE/4, 1987, Providence, RI.

[18] Correspondence between DiPippo, R., Bixley, P. F., and Gudmundsson, J. S. of the Department of Petroleum Engineering, Stanford University, Stanford, CA, 1987.